ACS Partner Journal
PRECISION CHEMISTRY
pubs.acs.org/PrecisionChem
Article

Photoresponsive Coatings by Light-Driven Molecular Motors in Cholesteric Liquid Crystal Microcapsules

Yan Wang,[§] Yang Zhang,[§] Shuhua Li, Wang Sun, Zhen Zhang, Guofu Zhou, Ben L. Feringa,* and Jiawen Chen*

Cite This: *Precis. Chem.* 2025, 3, 149−156

Read Online

ACCESS | Metrics & More | Article Recommendations | Supporting Information

ABSTRACT: Photoresponsive coatings that can change their color in response to light at ambient temperature have large potential applications. Cholesteric liquid crystals (CLCs) are promising photochromic materials, as they are known to reflect light selectively and their optical properties can be modulated with a wide range. However, it remains a major challenge to fabricate photoresponsive coatings that combine fast and good responsivity, fabrication feasibility, and mechanical strength and, more importantly, that can be applied at a large area with excellent stability. In this study, Pickering emulsions containing CLC microdroplets doped with light-driven molecular motors as photoresponsive chiral dopants were prepared via cellulose nanocrystals (CNCs) which serve as both Pickering emulsifiers and alignment agents of CLCs. A melamine−formaldehyde (MF) resin hybrid shell was fabricated via in situ polymerization to form thermally stable CLC microcapsules. These microcapsules were mixed with curable binders, resulting in photoresponsive coatings. The photochromic material which features highly selective addressability of the reflective light wavelength in the visible light region, good reversibility, and viewing angle independence was painted in a large area on both hard and soft substrates, providing a versatile platform for enhanced encryption and smart coatings.

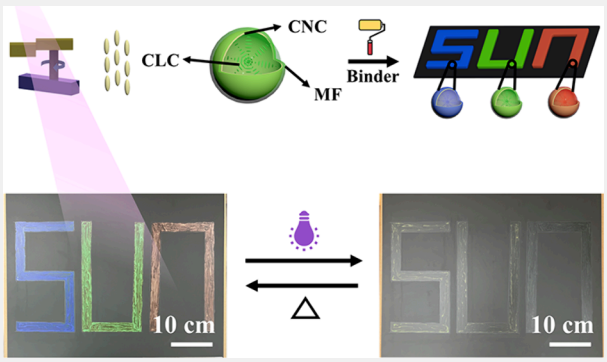

KEYWORDS: *photoresponsive coating, cholesteric liquid crystal, microcapsules, molecular motor, fast responsivity*

INTRODUCTION

Smart coatings that are photoresponsive and can change their color in response to light have promising applications.[1−3] Cholesteric liquid crystals (CLCs), as important photochromic materials, are great candidates to fabricate photoresponsive coatings. CLCs are able to selectively reflect light with a specific wavelength because of their periodic spiral structure, and their reflection band is controlled by the rotational pitch.[4−6] Therefore, photochromic chiral dopants that can adjust their molecular structures upon stimulus of light to induce a change of the helical pitch of CLCs are therefore considered as an important tool for dynamic modulation of optical properties of CLCs.[7−9] Illustrative examples of photochromic chiral dopants that are widely used include overcrowded alkenes,[10] azobenzene,[11−13] dithienylcyclopentene,[14,15] fulgide,[16,17] and spiroxamine derivatives.[18] Among these chiral dopants, light-driven molecular motors based on overcrowded alkenes provide unique features as, due to the intrinsic helicity, they undergo not only geometrical isomerization but axially helical changes as well during the rotary motion triggered by light and heat, allowing wide precision range control.[19,20] Motor-doped CLC's have enabled the discovery of rotating surfaces,[21−23] reconfigurable LC droplets,[24] supramolecular vortices,[25] adaptive optical materials[26,27] and soft actuators.[28,29] Our recent report has shown that CLC microdroplets containing light-driven molecular motor via capillary microfluidic technique provides angle independent rich structural color and fully reversible color tuning in the visible region.[30] Despite the excellent dynamic optical properties of motor-doped CLC microdroplets, the photoresponsive CLCs can flow and need to be filled or sealed into a cell structure, which significantly limits their practical application, especially when stable large area coating is required. The cross-linking of the CLC mixture can endow polymer films or coatings with good mechanical strength. However, the photochromic responsivity of CLCs is reduced or lost completely after cross-linking when the pitch is fixed.[31,32]

Received: December 26, 2024
Revised: February 16, 2025
Accepted: February 17, 2025
Published: March 5, 2025

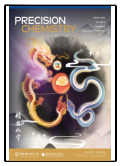

https://doi.org/10.1021/prechem.4c00103
Precis. Chem. 2025, 3, 149−156

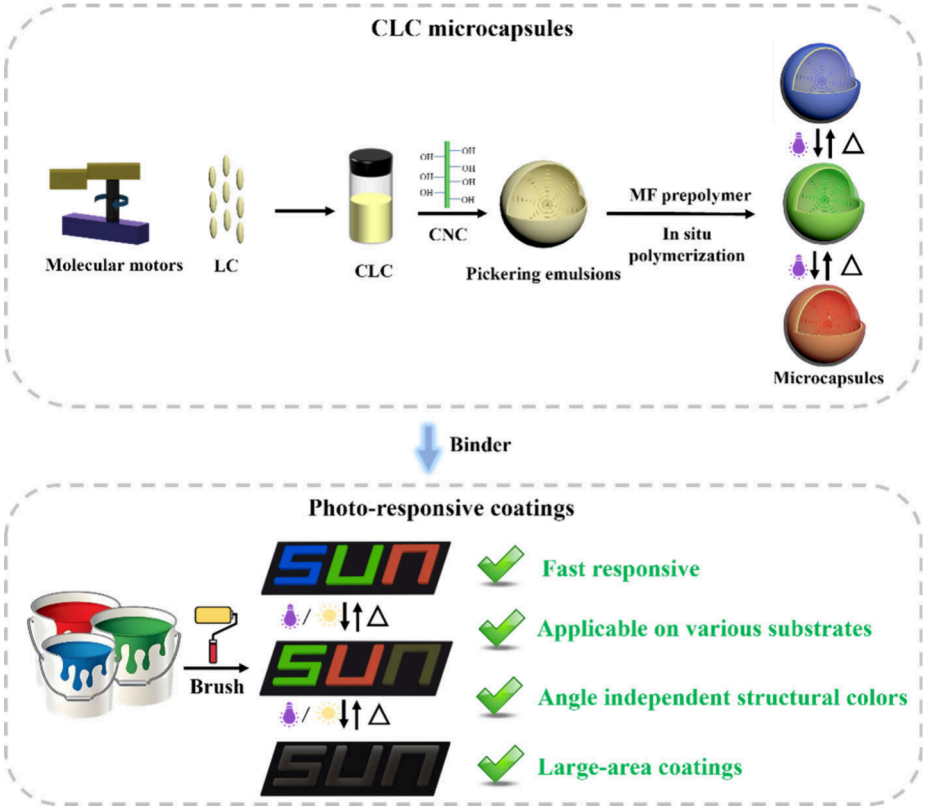

Figure 1. Representation of preparation and functioning of the photoresponsive coating based on molecular motor doped CLC microcapsules.

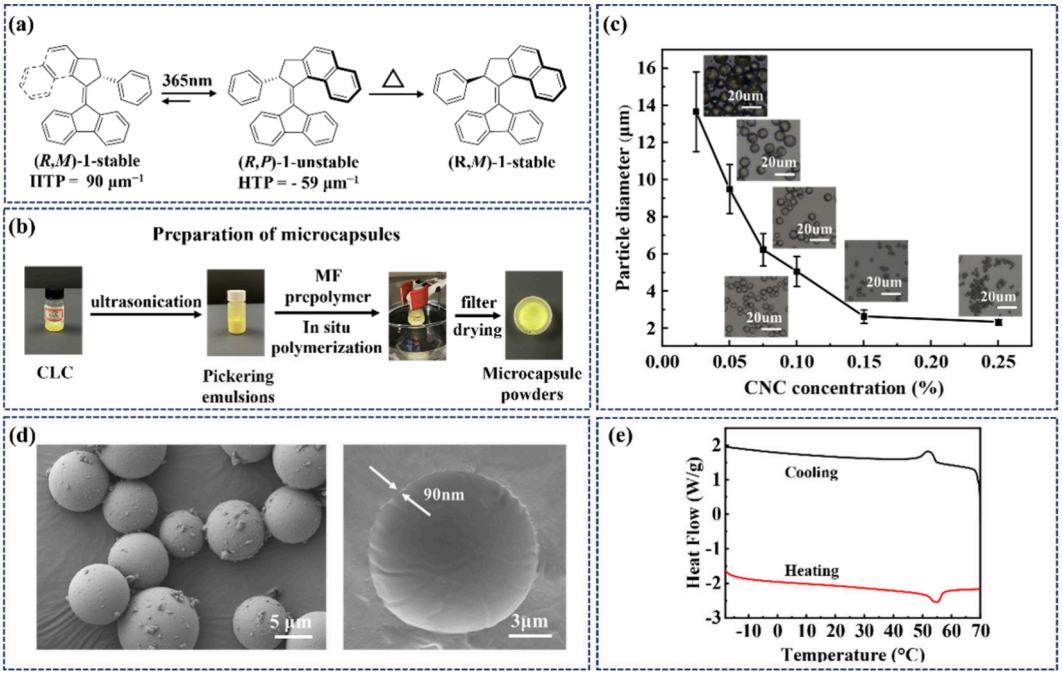

Figure 2. Preparation and morphology of CLC microcapsules containing motor **1**. (a) Unidirectional rotary cycle of the molecular motor **1**. (b) Real images of preparation process of CLC microcapsules. (c) Size of CLC droplets decreased when the concentration of CNCs was increased from 0.025 to 0.25 wt %. The inset in panel c shows the images of the CLC droplets under the microscope. (d) SEM images and (e) DSC curves of the CLC microcapsules.

We considered that a facile way to resolve these issues is by encapsulating a photoresponsive CLC mixture into a rigid shell, forming microcapsules. The CLC mixtures inside the microcapsules have to retain good photoresponsivity, and the rigid shells will prevent leakage of the CLCs and maintain a high mechanical strength. CLC microcapsules can then be fabricated into coatings by mixing with curable binders and brushing them on substrates. More importantly, the CLC

https://doi.org/10.1021/prechem.4c00103
Precis. Chem. 2025, 3, 149−156

microcapsule coatings are angle-independent due to the three-dimensional helical structure within the capsules. Several methods have been developed to fabricate the shells of CLC microcapsules using CLC emulsion microdroplets[33−36] as templates, such as in situ polymerization,[37,38] interfacial polymerization,[39,40] complex coacervation,[41,42] and solvent evaporation methods.[43] Compared to surfactant-stabilized conventional emulsions, solid-particle-stabilized Pickering emulsions show better stability and sustainability and have been demonstrated to be a promising template to fabricate microcapsules.[44−46] Cellulose nanocrystals (CNCs) are rodlike nanocelluloses and are normally extracted from wood pulp or cotton via acid hydrolysis.[47,48] Biorelated CNCs display outstanding Pickering emulsifying ability due to their partial wettability with both oil and water phases. CNC-stabilized Pickering emulsions are ideal templates to fabricate microcapsules due to the sustainability and biocompatibility of the CNCs, the excellent stability of the Pickering emulsions, and the good mechanical strength of the CNC-reinforced polymer shell.[49−51] CLC microcapsules with CNC-reinforced polymer shells have been reported recently.[52] By building on this strategy, we designed the photoresponsive coatings, embedding light-driven molecular motors based on CLC microcapsules via in situ polymerization of melamine-formaldehyde (MF). We discovered that the obtained photochromic materials show fast responsivity and angle independence and can be painted in a large area on both hard and soft substrates with excellent thermal stability (Figure 1).

RESULTS AND DISCUSSION

Preparation of Photoresponsive Microcapsules

Light-driven rotary motor molecule **1** was employed as the chiral dopant that is used to induce the formation of CLC (Figure 2a). According to our reported procedure,[21] both enantiomers of **1** can be prepared and separated at large scale and analyzed by chiral HPLC (Figure S1). (*R*,*M*)-stable-**1** adopts right-handed axial helicity and its helical twisting power is 90 μm^{-1} when used as chiral dopant in the LC material E7. When UV light is applied, it can undergo photoisomerization and results in the formation of the (*R*,*P*)-unstable-**1** isomer with opposite axial chirality, which induces a change of the HTP from 90 to −59 μm^{-1} (Figure 2a). When the irradiation is ceased, stable isomer (*R*,*M*)-**1** can be regenerated by a thermal helix inversion step, which completes the rotary cycle. The large variation in HTP value and the dynamic tuning of the chirality on demand during the rotary motion of **1** is key to modulation of optical properties of CLC.[7] Distinct from traditional LC thin film approaches, motor-doped CLCs are confined in the present study into spherical geometries, which allows to explore the LC microdroplets for their rich and angle-independent structural color.[53−55] The obtained CLC mixtures were mixed with water-dispersed CNCs and NaCl solution to form Pickering emulsions by ultrasonication employing a cell disruptor (for a detailed procedure, see Supporting Information). A sample with a concentration of 0.025 wt % CNCs was prepared and studied under polarized optical microscopy (POM) (Figure S2). It is shown that all the CLC droplets displayed a Maltese cross between two crossed polarizers, indicating that the CLC inside the droplets adopt a centrosymmetric parallel orientation with a radially distributed helical axis and good alignment.[35,56] However, the distribution of the CLC microdroplets size was found to be wide, from 6 to 24 μm (Figure S3). The large size of the microdroplets is not preferred as demulsification can occur.[57] Therefore, a variety of concentrations of CNCs (Figure 2c and Table S1) were screened to tune the size of the CLC microdroplets. As shown in Figure 2c, when the concentration of CNCs was increased from 0.025 to 0.25 wt %, the averaged size of microdroplets was reduced significantly from 13.9 to 2.8 μm. The reason is that CNCs serve as emulsifiers in the present study, and increasing their amount can stabilize a larger interface area, resulting in stable liquid crystal droplets with smaller size.[49] The microdroplets of smaller size showed a more obvious Maltese cross than those of larger size, indicating a more orderly orientation of the LC mesogenic units that may lead to better reflectance (Figure S2). However, when the diameter of the CLC droplets is reduced only a small number of pitches form inside, resulting in reduced reflection. Therefore, after comprehensively considering the size and reflectance properties, 0.05 wt % CNCs was employed. Furthermore, the size and uniformity of CLC droplets were affected by ultrasonic time as well. Under the fix concentration of CNCs and sonication power, different preparation times were studied. As shown in Figure S4, when the ultrasonic time was set to be 2 min, it was found that the size distribution range became narrow, and the average particle size of CLC droplets is 9.5 μm. When the ultrasonic time was extended, the size distribution of CLC microdroplets became wider and the average particle size became too small. Based on the above experimental results, an average diameter of 9.5 μm CLC droplets prepared via a CNCs concentration of 0.05 wt %, and an ultrasonic time of 2 min was selected for the remainder of this study.

As the CNC-stabilized CLC microdroplets are not stable in the dry state, a rigid shell that can cover the outside of the CNC layer is required when the droplets are exposed to air.[52,57] We considered a MF resin provides an ideal material to serve as the shell of the droplets as it is known for its easy preparation, high mechanical strength and thermal stability.[37] The MF prepolymer trihydroxy methyl melamine was generated via a Schiff base reaction between formaldehyde and melamine (Scheme S1). Then MF prepolymers were further polymerized and cross-linked on the surface of the CLC droplets via in situ polymerization, resulting in CLC microcapsules. The obtained CLC microcapsules were first studied by scanning electrical microscopy. Figure 2d shows that the spherical morphology of the CLC droplet remained intact after covering the outside with an MF shell whose thickness was found to be 90 nm (Figure S5). In order to test the thermal stability of the prepared microcapsules, the same sample was measured again after one-year storage in open air and an SEM image reveals the preserved spherical morphology of the CLC microcapsules (Figure S5). In addition, differential scanning calorimetry measurement shows that the phase transition temperature of the obtained microcapsule is 54 °C which indicates its stability at room temperature (rt, Figure 2e). Furthermore, the prepared CLC microcapsules were studied by thermogravimetric analysis, as shown in Figure S6. The sample is stable below 200 °C, showing excellent thermal stability and its feasibility for our daily life application.

Photoresponsive Behavior of CLC Microcapsules

When a light-driven molecular motor **1** is embedded in the CLC microcapsule, it is expected that when UV irradiation is applied, the rotation motion of motor **1** that is accompanied by the change of the axial helicity can induce the tuning of HTP

https://doi.org/10.1021/prechem.4c00103
Precis. Chem. 2025, 3, 149−156

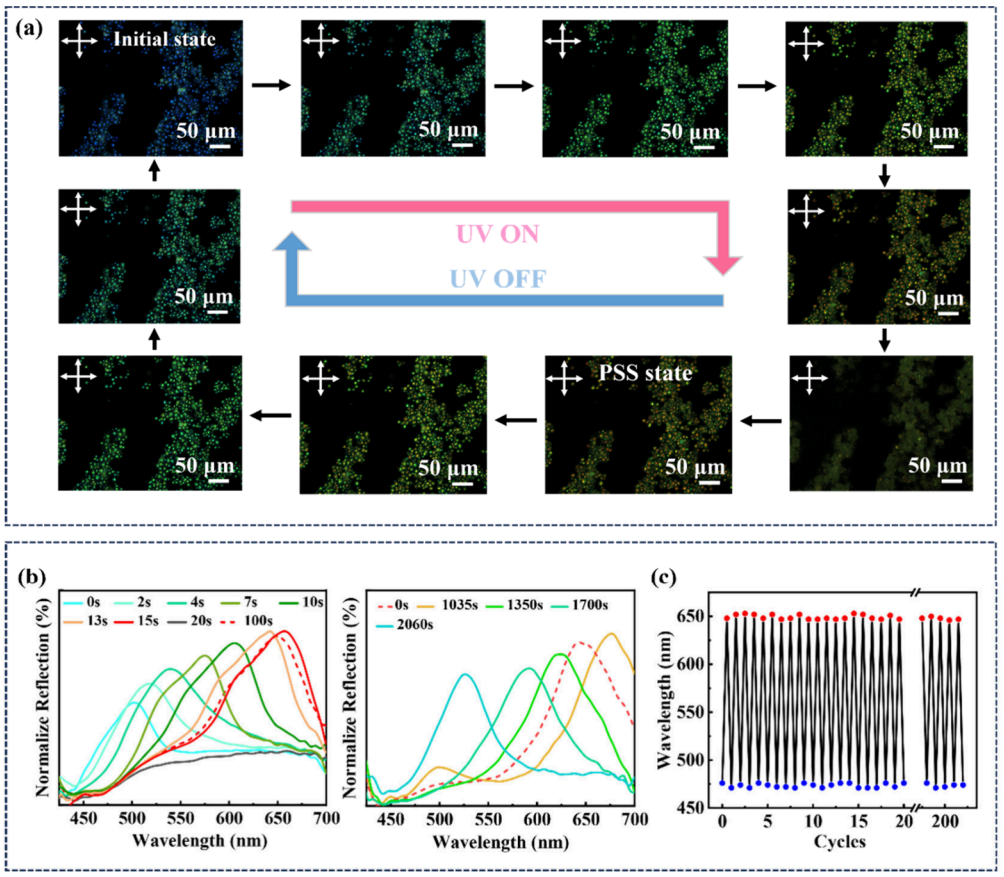

Figure 3. (a) POM images and (b) reflection spectra of the CLC microcapsules at different irradiation times. (c) Shift in the reflection band of the microcapsules during 200 cycles of UV irradiation.

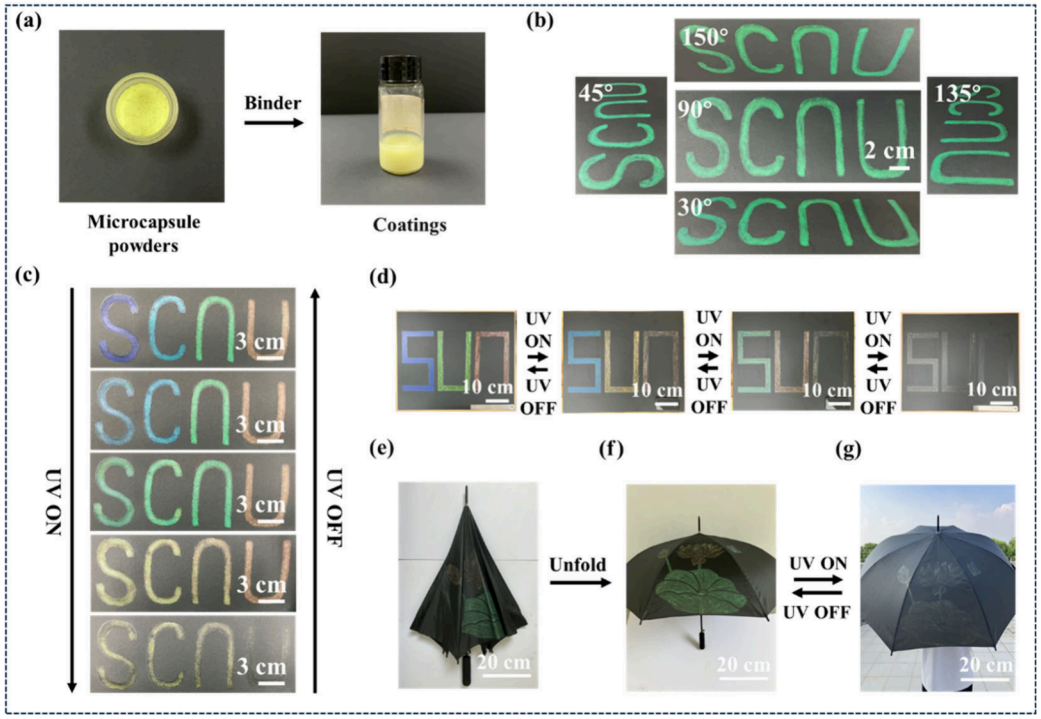

Figure 4. Photoresponsive coating. (a) Real images of the process of preparation of a coating from the micropause. (b) Photoresponsive coating shown at different viewing angles. (c) Changes of a "SCNU" coating before and after local UV irradiation. (d) Coating painted on the hard substrate. A pattern of a lotus leaf was painted on the umbrella in the (e) fold state and (f) open state. (g) Color change of the pattern on the umbrella under the natural light.

https://doi.org/10.1021/prechem.4c00103
Precis. Chem. 2025, 3, 149−156

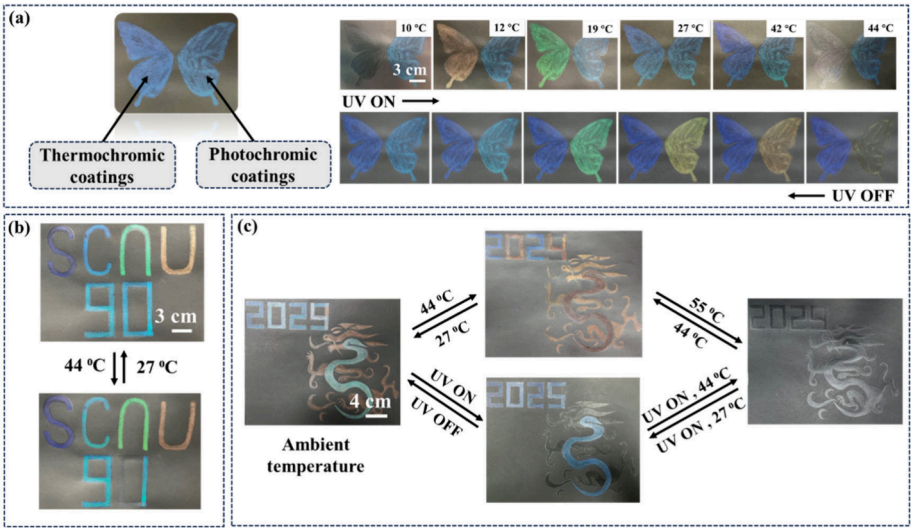

Figure 5. Dynamic coating pattern. Color changes of (a) butterfly patterns, (b) message "SCNU 90", and (c) the dragon or snake pattern and numbers prepared on the basis of thermochromic coating and photochromic coating under temperature and light stimulation.

of the CLC, therefore resulting in the change of the reflective color. Figure 3a shows POM images of microcapsules containing 4.02 wt % (*R*,*M*)-**1**. The single blue reflective color located at the core of the sphere confirms the proper orientation of the motor and LC molecules and shows that the helical axes are radially aligned and perpendicular to the surface within the droplets, which is key to the optically angle independent property. Upon UV irradiation, the initial blue color showed a red shift, according to Bragg's law, due to the decrease of HTP originated from the formation of (*R*,*P*)-unstable-**1**. When the motor reached the photostationary state (PSS) (Figure 3a), the microcapsule showed a red-shifted reflective color. After stopping irradiation, the superstructure of CLC gradually regenerated to the original state, concomitant with the central color changing from red to the initial blue. In order to study the details during the change of color, the central reflective wavelength was followed quantitatively in time. During the irradiation (365 nm, 5 mW/cm^2), it shifted from 500 to 650 nm within 15 s and finally to 648 nm after 100 s when motor **1** reached PSS (Figure 3b). When the irradiation stopped, the central reflective color showed a gradual blue shift, from 648 nm to the original 500 nm after 2060 s. Microcapsules with different initial central colors can be obtained by doping (*R*,*M*)-**1** with different concentrations and the corresponding change of color upon irradiation was monitored and detailed as shown in the Supporting Information (Figure S7 and 3b). Furthermore, the dynamic color modulation of these thermally stable microcapsules was tested over more than 200 cycles, and significant fatigue was not observed (Figure 3c), setting a solid base of these photochromic microcapsules for practical applications.

Photoresponsive Coatings

In order to prepare photoresponsive coatings, a commercial transparent water-based binder (water glue, refractive index 1.45, mainly composed of PVA) was chosen as the matrix of CLC microcapsules. The green CLC microcapsules doped with 3.29 wt % (*R*,*M*)-**1** were mixed with the binder by a weight ratio of 1:25. The resulting coating was subsequently painted on the substrate and dried under ambient conditions for 20 min (Figure 4a). The obtained letter "SCNU" showed bright green colors (Figure 4b). More importantly, the structurally defined spherical CLCs provide angle-independent structural color as shown in Figure 4b. The rich green color is well preserved when viewing from different angles. Next, four different initial colors of photochromic coatings: dark blue, light blue, green, and red were prepared, respectively. They were brushed on a hard substrate, i.e., plastic, to write the letters "SCNU", as shown in Figure 4c. UV irradiation was first applied to the letter "S", turning its color from dark blue to light blue, which is the same color as letter "C" (Figure 4c). Then the UV light was illuminated on both letters "S" and "C" pushing their color from light blue to green, resulting in the same color of "SCN" (Figure 4c). Subsequently, UV irradiation was applied on all letters "SCNU" that lead to the reflective color at the near-infrared region. The weak red reflective color was suppressed by motor's pigment color, showing pale-yellow letters (Figure 4c). When the UV irradiation was stopped, the original color could be regained within 20 min, and the process is fully reversible.

Next, the obtained photoresponsive coatings were painted in large areas on both hard and soft substrates. Three different initial colors, blue, green, and red, were painted on a rigid black acrylic plate with a size of 50 × 60 cm^2, as shown in Figure 4d. When the plate was brought outdoors and placed in direct sunlight, the bright structural colors of letters "SUN" disappeared within 2 min (Figure 4d), leaving a pale-yellow color. Next, when the plate was put indoors, the original colors could be restored within 20 min. In addition, a "summer lotus" pattern was painted on the flexible fabric surface of an umbrella. The "lotus leaf" was painted by green coatings, the "flower" was painted by red color, and the "butterfly" was used with blue coating. Panels e and f of Figure 4 show that when the umbrella is folded or opened, the color of the pattern remains consistent. The whole pattern disappeared when the umbrella was brought outdoors in sunlight (Figure 4g) and could be regenerated after placing the umbrella indoors. It is worth noting that the patterns that are drawn on the flexible surface of the umbrella show bright rich color and fast and good switching reversibility after more than 100 cycles, which is crucial for further application in color-changing decoration and artificial skins.[58,59]

https://doi.org/10.1021/prechem.4c00103
Precis. Chem. 2025, 3, 149−156

With these photoresponsive coatings in hand, we decided to employ thermochromic coatings doped with thermal responsive CLC microcapsules to achieve more complex dynamic patterns. According to a previously reported procedure,[52] thermally responsive CLC coatings containing S811 and S5011 as chiral dopants were prepared. The operating temperatures of these coatings are 12−42 °C. When the temperature is increased, a blue shift can occur. The colors are red, green, light blue, and blue at 12, 19, 27, and 42 °C, respectively. When the temperature is below 12 °C, the material reaches the smectic phase and becomes transparent. When the temperature is above 44 °C, it reaches an isotropic state, and the structural color disappears as well. A colorful butterfly was drawn on a black cardboard, as shown in Figure 5a. The left wing was painted with thermal-responsive CLC coatings, and the right wing has a photochromic coating doped with 3.86 wt % (*R*,*M*)-**1**. At rt indoor, both left and right wings show a light blue color (Figure 5a). When the temperature gradually was increased to 42 °C or decreased to 12 °C, the color of the left wing showed a blue or red shift, respectively, while keeping the color of the right wing intact (Movie S1). Alternatively, when the black board was brought outdoors in the sunlight, the blue color of the right wing changed to green within 10 s and finally reached a pale-yellow color after 2 min (Movie S2). The blue color of the left wing remained unchanged. The initial blue color could be regained when the board was placed indoors. In addition, when the board was heated during the irradiation, both of the colors of left and right wings changed accordingly, showing no cross-talk to each other. It is important to note that the thermo- and photoresponsive coatings that are used in the present study can function orthogonally. Therefore, multiple layers were tested for information storage and encryption. Figure 5b shows the letters "SCNU" with 4 different colors prepared by photoresponsive CLC coatings. The number "9" is painted by light blue photoresponsive coatings. The number "0" is initially painted with a thermochromic coating, followed by an additional layer of light-responsive coating applied to the right half of number "0". At rt, the message "SCNU 90" was shown, representing the 90 anniversaries of the SCNU university. The temperature is heated to or above 44 °C, which is the clearing point of CLC of the thermochromic coatings, and the structural color disappears. As the clearing point of photoresponsive CLC coating is 55 °C (Figure 2e), it retained the original blue color, and therefore the information was converted from "SCNU 90" to "SCNU 91" (Figure 5b). Furthermore, a Chinese zodiac drawing was prepared on the surface (Figure 5c). Blue and red photoresponsive coatings were used to paint the bottom layer of number "2024" and the pattern "Dragon", respectively, as the bottom layer. Subsequently, thermal responsive coatings were painted on top of the numbers "2024" and "0" as well as part of the dragon pattern. Meanwhile, further informatio, i.e., the numbers "0" and "5", and a snake-shaped pattern were painted as well. After being dried at rt for 20 min, a smart Chinese zodiac card was prepared. At rt, chaotic information was observed as it is due to mixing of two layers of patterns (Figure 5c). When the card was placed below 12 °C or between 44 and 55 °C, the structural color of thermochromic coatings disappeared and information "2024 Dragon" could be read out. Alternatively, when the card was irradiated with UV light or brought outdoors in the sunlight at rt, the structural color of the bottom layer, i.e., photoresponsive coatings, disappeared and message "2025 Snake" was shown (Figure 5c). Further heating of the card in outdoor sunlight led to the complete erasure of the whole pattern. More importantly, each state of the smart zodiac card can be addressed precisely and is fully reversible.

CONCLUSIONS

In conclusion, we present here a facile way to fabricate photoresponsive coatings that can be painted in a large area on both hard and soft substrates. CLCs doped with a light-driven molecular motor as a chiral dopant were mixed with CNCs to form Pickering emulsions. The size of the CLC Pickering emulsion droplets can be well tuned using the different concentrations of CNCs, and CLC droplets with diameters of about 10 μm were preferred due to their high reflectance and orderly alignment. The droplets were covered with a solid shell by in situ polymerization of MF precursors, resulting in CLC microcapsules that show long-term stability in air. The microcapsules were subsequently mixed with curable glue to generate photoresponsive coatings, which can be painted on various substrates. The coatings showed rich and bright structural color, fast responsivity to UV irradiation, precise addressability of specific reflective wavelength of visible light, and angle independence. In addition, a combination of photo- and thermoresponsive coatings resulted in complex patterns in which dual information can be selectively read out. Our approach of preparing photoresponsive coatings provides major potential toward advanced smart decorative coatings and high-level encryption.

ASSOCIATED CONTENT

Supporting Information

The Supporting Information is available free of charge at https://pubs.acs.org/doi/10.1021/prechem.4c00103.

Experimental methods, HPLC spectroscopy, POM images of CLC droplets, particle size distribution of CLC droplets, mechanism of in situ polymerization to form microcapsules, SEM images and TGA curves of CLC microcapsules, POM images of color change of CLC microcapsules under UV irradiation (PDF)

Movie S1 showing the color change of the dynamic butterfly pattern at different temperatures (AVI)

Movie S2 showing the color change of the dynamic butterfly pattern under natural light (AVI)

AUTHOR INFORMATION

Corresponding Authors

Ben L. Feringa − *SCNU-UG International Joint Laboratory of Molecular Science and Display, South China Normal University, Guangzhou 510006, China; Stratingh Institute for Chemistry, University of Groningen, 9747AG Groningen, The Netherlands;* orcid.org/0000-0003-0588-8435; Email: b.l.feringa@rug.nl

Jiawen Chen − *SCNU-UG International Joint Laboratory of Molecular Science and Display, South China Normal University, Guangzhou 510006, China;* orcid.org/0000-0003-1233-5599; Email: j.chen@m.scnu.edu.cn

Authors

Yan Wang − *SCNU-UG International Joint Laboratory of Molecular Science and Display, South China Normal University, Guangzhou 510006, China*

Yang Zhang − *SCNU-UG International Joint Laboratory of Molecular Science and Display, South China Normal University, Guangzhou 510006, China;* orcid.org/0000-0002-9796-0790
Shuhua Li − *SCNU-UG International Joint Laboratory of Molecular Science and Display, South China Normal University, Guangzhou 510006, China*
Wang Sun − *SCNU-UG International Joint Laboratory of Molecular Science and Display, South China Normal University, Guangzhou 510006, China*
Zhen Zhang − *SCNU-UG International Joint Laboratory of Molecular Science and Display, South China Normal University, Guangzhou 510006, China;* orcid.org/0000-0002-9704-6472
Guofu Zhou − *SCNU-UG International Joint Laboratory of Molecular Science and Display, South China Normal University, Guangzhou 510006, China;* orcid.org/0000-0003-1101-1947

Complete contact information is available at: https://pubs.acs.org/10.1021/prechem.4c00103

Author Contributions

[§]Y.W. and Y.Z. contributed equally to this work.

Notes

The authors declare no competing financial interest.

■ ACKNOWLEDGMENTS

This work was supported financially by the National Key R&D Program of China (2020YFE0100200), Guangdong Basic and Applied Basic Research Foundation (2024A1515010687), Science and Technology Projects in Guangzhou (202201000008), and Guangdong Provincial Key Laboratory of Optical Information Materials and Technology (No. 2023B1212060065), and The Netherlands Ministry of Education, Culture and Science (Gravitation Program 024.001.035 to B.L.F.).

■ REFERENCES

(1) Lan, R.; Bao, J.; Huang, R.; Wang, Z.; Zhang, L.; Shen, C.; Wang, Q.; Yang, H. Amplifying Molecular Scale Rotary Motion: The Marriage of Overcrowded Alkene Molecular Motor with Liquid Crystals. *Adv. Mater.* **2022**, *34* (40), 2109800.
(2) Xu, L.; Mou, F.; Gong, H.; Luo, M.; Guan, J. Light-Driven Micro/Nanomotors: From Fundamentals to Applications. *Chem. Soc. Rev.* **2017**, *46* (22), 6905−6926.
(3) Bhatti, M. R. A.; Kernin, A.; Tausif, M.; Zhang, H.; Papageorgiou, D.; Bilotti, E.; Peijs, T.; Bastiaansen, C. W. M. Light-Driven Actuation in Synthetic Polymers: A Review from Fundamental Concepts to Applications. *Adv. Opt. Mater.* **2022**, *10* (10), 2102186.
(4) Bisoyi, H. K.; Li, Q. Light-Driven Liquid Crystalline Materials: From Photo-Induced Phase Transitions and Property Modulations to Applications. *Chem. Rev.* **2016**, *116* (24), 15089−15166.
(5) Wang, L.; Urbas, A. M.; Li, Q. Nature-Inspired Emerging Chiral Liquid Crystal Nanostructures: From Molecular Self-Assembly to DNA Mesophase and Nanocolloids. *Adv. Mater.* **2020**, *32* (41), 1801335.
(6) McConney, M. E.; Rumi, M.; Godman, N. P.; Tohgha, U. N.; Bunning, T. J. Photoresponsive Structural Color in Liquid Crystalline Materials. *Adv. Opt. Mater.* **2019**, *7* (16), 1900429.
(7) Lan, R.; Bao, J.; Huang, R.; Wang, Z.; Zhang, L.; Shen, C.; Wang, Q.; Yang, H. Amplifying Molecular Scale Rotary Motion: The Marriage of Overcrowded Alkene Molecular Motor with Liquid Crystals. *Adv. Mater.* **2022**, *34* (40), 2109800.
(8) He, Z.; Cheng, X.; Wang, Z.; Zhang, W. Chiral Structures in Azobenzene-containing Systems: Construction, Regulation, and Application. *Responsive Mater.* **2024**, *2* (2), No. e20240010.
(9) Wang, Y.; Li, Q. Light-Driven Chiral Molecular Switches or Motors in Liquid Crystals. *Adv. Mater.* **2012**, *24* (15), 1926−1945.
(10) Feringa, B. L.; Huck, N. P. M.; Van Doren, H. A. Chiroptical Switching between Liquid Crystalline Phases. *J. Am. Chem. Soc.* **1995**, *117* (39), 9929−9930.
(11) Kim, Y.; Tamaoki, N. Asymmetric Dimers of Chiral Azobenzene Dopants Exhibiting Unusual Helical Twisting Power upon Photoswitching in Cholesteric Liquid Crystals. *ACS Appl. Mater. Interfaces* **2016**, *8* (7), 4918−4926.
(12) Ikeda, T.; Tsutsumi, O. Optical Switching and Image Storage by Means of Azobenzene Liquid-Crystal Films. *Science* **1995**, *268* (5219), 1873−1875.
(13) Wang, H.; Bisoyi, H. K.; Urbas, A.; Bunning, T. J.; Li, Q. Reversible Circularly Polarized Reflection in a Self-Organized Helical Superstructure Enabled by a Visible Light-Driven Axially Chiral Molecular Switch. *J. Am. Chem. Soc.* **2019**, *141* (20), 8078−8082.
(14) Zheng, Z.; Hu, H.; Zhang, Z.; Liu, B.; Li, M.; Qu, D.-H.; Tian, H.; Zhu, W.-H.; Feringa, B. L. Digital Photoprogramming of Liquid-Crystal Superstructures Featuring Intrinsic Chiral Photoswitches. *Nat. Photonics* **2022**, *16* (3), 226−234.
(15) Zheng, Z.; Li, Y.; Bisoyi, H. K.; Wang, L.; Bunning, T. J.; Li, Q. Three-Dimensional Control of the Helical Axis of a Chiral Nematic Liquid Crystal by Light. *Nature* **2016**, *531* (7594), 352−356.
(16) Janicki, S. Z.; Schuster, G. B. A Liquid Crystal Opto-Optical Switch: Nondestructive Information Retrieval Based on a Photochromic Fulgide as Trigger. *J. Am. Chem. Soc.* **1995**, *117* (33), 8524−8527.
(17) White, T. J.; Zhao, A. D.; Cazzell, S. A.; Bunning, T. J.; Kosa, T.; Sukhomlinova, L.; Smith, T. J.; Taheri, B. Optically Reconfigurable Color Change in Chiral Nematic Liquid Crystals Based on Indolylfulgide Chiral Dopants. *J. Mater. Chem.* **2012**, *22* (12), 5751.
(18) Jin, L.-M.; Li, Y.; Ma, J.; Li, Q. Synthesis of Novel Thermally Reversible Photochromic Axially Chiral Spirooxazines. *Org. Lett.* **2010**, *12* (15), 3552−3555.
(19) Koumura, N.; Zijlstra, R. W. J.; Van Delden, R. A.; Harada, N.; Feringa, B. L. Light-Driven Monodirectional Molecular Rotor. *Nature* **1999**, *401* (6749), 152−155.
(20) Koumura, N.; Geertsema, E. M.; van Gelder, M. B.; Meetsma, A.; Feringa, B. L. Second Generation Light-Driven Molecular Motors. Unidirectional Rotation Controlled by a Single Stereogenic Center with Near-Perfect Photoequilibria and Acceleration of the Speed of Rotation by Structural Modification. *J. Am. Chem. Soc.* **2002**, *124* (18), 5037−5051.
(21) Eelkema, R.; Pollard, M. M.; Vicario, J.; Katsonis, N.; Ramon, B. S.; Bastiaansen, C. W. M.; Broer, D. J.; Feringa, B. L. Nanomotor Rotates Microscale Objects. *Nature* **2006**, *440* (7081), 163−163.
(22) Bosco, A.; Jongejan, M. G. M.; Eelkema, R.; Katsonis, N.; Lacaze, E.; Ferrarini, A.; Feringa, B. L. Photoinduced Reorganization of Motor-Doped Chiral Liquid Crystals: Bridging Molecular Isomerization and Texture Rotation. *J. Am. Chem. Soc.* **2008**, *130* (44), 14615−14624.
(23) Eelkema, R.; Pollard, M. M.; Katsonis, N.; Vicario, J.; Broer, D. J.; Feringa, B. L. Rotational Reorganization of Doped Cholesteric Liquid Crystalline Films. *J. Am. Chem. Soc.* **2006**, *128* (44), 14397−14407.
(24) Orlova, T.; Lancia, F.; Loussert, C.; Iamsaard, S.; Katsonis, N.; Brasselet, E. Revolving Supramolecular Chiral Structures Powered by Light in Nanomotor-Doped Liquid Crystals. *Nat. Nanotechnol.* **2018**, *13* (4), 304−308.
(25) Chen, J.; Lacaze, E.; Brasselet, E.; Harutyunyan, S. R.; Katsonis, N.; Feringa, B. L. Textures of Cholesteric Droplets Controlled by Photo-Switching Chirality at the Molecular Level. *J. Mater. Chem. C* **2014**, *2* (38), 8137−8141.
(26) Hou, J.; Mondal, A.; Long, G.; De Haan, L.; Zhao, W.; Zhou, G.; Liu, D.; Broer, D. J.; Chen, J.; Feringa, B. L. Photo-responsive

Helical Motion by Light-Driven Molecular Motors in a Liquid-Crystal Network. *Angew. Chem., Int. Ed.* **2021**, *60* (15), 8251−8257.
(27) Hou, J.; Long, G.; Zhao, W.; Zhou, G.; Liu, D.; Broer, D. J.; Feringa, B. L.; Chen, J. Phototriggered Complex Motion by Programmable Construction of Light-Driven Molecular Motors in Liquid Crystal Networks. *J. Am. Chem. Soc.* **2022**, *144* (15), 6851−6860.
(28) Ryabchun, A.; Lancia, F.; Chen, J.; Morozov, D.; Feringa, B. L.; Katsonis, N. Helix Inversion Controlled by Molecular Motors in Multistate Liquid Crystals. *Adv. Mater.* **2020**, *32* (47), 2004420.
(29) White, T. J.; Cazzell, S. A.; Freer, A. S.; Yang, D.-K.; Sukhomlinova, L.; Su, L.; Kosa, T.; Taheri, B.; Bunning, T. J. Widely Tunable, Photoinvertible Cholesteric Liquid Crystals. *Adv. Mater.* **2011**, *23* (11), 1389−1392.
(30) Li, J.; Xie, S.; Meng, J.; Liu, Y.; Zhan, Q.; Zhang, Y.; Shui, L.; Zhou, G.; Feringa, B. L.; Chen, J. Dynamic Control of Multiple Optical Patterns of Cholesteric Liquid Crystal Microdroplets by Light-Driven Molecular Motors. *CCS Chem.* **2024**, *6* (2), 427−438.
(31) Zhang, W.; Kragt, S.; Schenning, A. P. H. J.; de Haan, L. T.; Zhou, G. Easily Processable Temperature-Responsive Infrared-Reflective Polymer Coatings. *ACS Omega* **2017**, *2* (7), 3475−3482.
(32) Pallares, R. M.; Su, X.; Lim, S. H.; Thanh, N. T. K. Fine-Tuning of Gold Nanorod Dimensions and Plasmonic Properties Using the Hofmeister Effects. *J. Mater. Chem. C* **2016**, *4* (1), 53−61.
(33) Park, N.-H.; Park, S.-I.; Suh, K.-D. A Novel Method for Encapsulation of a Liquid Crystal in Monodisperse Micron-Sized Polymer Particles. *Colloid & Polymer Science* **2001**, *279* (11), 1082−1089.
(34) Lin, P.; Yan, Q.; Wei, Z.; Chen, Y.; Chen, S.; Wang, H.; Huang, Z.; Wang, X.; Cheng, Z. Chiral Photonic Crystalline Microcapsules with Strict Monodispersity, Ultrahigh Thermal Stability, and Reversible Response. *ACS Appl. Mater. Interfaces* **2018**, *10* (21), 18289−18299.
(35) Belmonte, A.; Bus, T.; Broer, D. J.; Schenning, A. P. H. J. Patterned Full-Color Reflective Coatings Based on Photonic Cholesteric Liquid-Crystalline Particles. *ACS Appl. Mater. Interfaces* **2019**, *11* (15), 14376−14382.
(36) Lee, S. S.; Kim, J. B.; Kim, Y. H.; Kim, S.-H. Wavelength-Tunable and Shape-Reconfigurable Photonic Capsule Resonators Containing Cholesteric Liquid Crystals. *Sci. Adv.* **2018**, *4* (6), No. eaat8276.
(37) Hu, X.; Huang, Z.; Zhang, Y. Preparation of CMC-Modified Melamine Resin Spherical Nano-Phase Change Energy Storage Materials. *Carbohydr. Polym.* **2014**, *101*, 83−88.
(38) Ju, H.-K.; Kim, J.-W.; Han, S.-H.; Chang, I.-S.; Kim, H.-K.; Kang, H.-H.; Lee, O.-S.; Suh, K.-D. Thermotropic Liquid-Crystal/Polymer Microcapsules Prepared by in Situ Suspension Polymerization. *Colloid & Polymer Science* **2002**, *280* (10), 879−885.
(39) Liu, H.; Jiang, M.; Geng, S.; Liu, X. Modulation of an Si-O-Si Structure in Uniformly Photochromic Microcapsules for Solar Heat and Daylight Management. *Chem. Eng. J.* **2024**, *490*, 151545.
(40) Hong, K.; Park, S. Preparation of Polyurea Microcapsules with Different Composition Ratios: Structures and Thermal Properties. *Mater. Sci. Eng. A-struct.* **1999**, *272* (2), 418−421.
(41) Rong, Y.; Chen, H.-Z.; Wei, D.-C.; Sun, J.-Z.; Wang, M. Microcapsules with Compact Membrane Structure from Gelatin and Styrene-Maleic Anhydride Copolymer by Complex Coacervation. *Colloid Surface A* **2004**, *242* (1−3), 17−20.
(42) Huang, R.; Lan, R.; Shen, C.; Zhang, Z.; Wang, Z.; Bao, J.; Wang, Z.; Zhang, L.; Hu, W.; Yu, Z.; Zhu, S.; Wang, L.; Yang, H. Remotely Controlling Drug Release by Light-Responsive Cholesteric Liquid Crystal Microcapsules Triggered by Molecular Motors. *ACS Appl. Mater. Interfaces* **2021**, *13* (49), 59221−59230.
(43) Sheng, M.; Li, J.; Jiang, X.; Wang, C.; Li, J.; Zhang, L.; Fu, S. Biomimetic Solid-Liquid Transition Structural Dye-Doped Liquid Crystal/Phase-Change-Material Microcapsules Designed for Wearable Bistable Electrochromic Fabric. *ACS Appl. Mater. Interfaces* **2021**, *13* (28), 33282−33290.
(44) Choi, Y. H.; Lee, S. S.; Lee, D.; Jeong, H. S.; Kim, S. Composite Microgels Created by Complexation between Polyvinyl Alcohol and Graphene Oxide in Compressed Double-Emulsion Drops. *Small* **2020**, *16* (9), 1903812.
(45) Tang, C.; Chen, Y.; Luo, J.; Low, M. Y.; Shi, Z.; Tang, J.; Zhang, Z.; Peng, B.; Tam, K. C. Pickering Emulsions Stabilized by Hydrophobically Modified Nanocellulose Containing Various Structural Characteristics. *Cellulose* **2019**, *26*, 7753−7767.
(46) Guan, Y.; Zhang, L.; Wang, D.; West, J. L.; Fu, S. Preparation of Thermochromic Liquid Crystal Microcapsules for Intelligent Functional Fiber. *Materials & Design* **2018**, *147*, 28−34.
(47) Zhang, Z.; Tam, K. C.; Wang, X.; Sèbe, G. Inverse Pickering Emulsions Stabilized by Cinnamate Modified Cellulose Nanocrystals as Templates To Prepare Silica Colloidosomes. *ACS Sustainable Chem. Eng.* **2018**, *6* (2), 2583−2590.
(48) Wang, P.-X.; Hamad, W. Y.; MacLachlan, M. J. Structure and Transformation of Tactoids in Cellulose Nanocrystal Suspensions. *Nat. Commun.* **2016**, *7* (1), 11515.
(49) Zhang, B.; Zhang, Z.; Kapar, S.; Ataeian, P.; Da Silva Bernardes, J.; Berry, R.; Zhao, W.; Zhou, G.; Tam, K. C. Microencapsulation of Phase Change Materials with Polystyrene/Cellulose Nanocrystal Hybrid Shell via Pickering Emulsion Polymerization. *ACS Sustainable Chem. Eng.* **2019**, *7* (21), 17756−17767.
(50) Zhang, Z.; Cheng, M.; Gabriel, M. S.; Teixeira Neto, Â. A.; Da Silva Bernardes, J.; Berry, R.; Tam, K. C. Polymeric Hollow Microcapsules (PHM) via Cellulose Nanocrystal Stabilized Pickering Emulsion Polymerization. *J. Colloid Interface Sci.* **2019**, *555*, 489−497.
(51) Zhu, W.; Ma, W.; Li, C.; Pan, J.; Dai, X. Well-Designed Multihollow Magnetic Imprinted Microspheres Based on Cellulose Nanocrystals (CNCs) Stabilized Pickering Double Emulsion Polymerization for Selective Adsorption of Bifenthrin. *Chem. Eng. J.* **2015**, *276*, 249−260.
(52) Yang, T.; Yuan, D.; Liu, W.; Zhang, Z.; Wang, K.; You, Y.; Ye, H.; De Haan, L. T.; Zhang, Z.; Zhou, G. Thermochromic Cholesteric Liquid Crystal Microcapsules with Cellulose Nanocrystals and a Melamine Resin Hybrid Shell. *ACS Appl. Mater. Interfaces* **2022**, *14* (3), 4588−4597.
(53) Cipparrone, G.; Mazzulla, A.; Pane, A.; Hernandez, R. J.; Bartolino, R. Chiral Self-Assembled Solid Microspheres: A Novel Multifunctional Microphotonic Device. *Adv. Mater.* **2011**, *23* (48), 5773−5778.
(54) Uchida, Y.; Takanishi, Y.; Yamamoto, J. Controlled Fabrication and Photonic Structure of Cholesteric Liquid Crystalline Shells. *Adv. Mater.* **2013**, *25* (23), 3234−3237.
(55) Aβhoff, S. J.; Sukas, S.; Yamaguchi, T.; Hommersom, C. A.; Le Gac, S.; Katsonis, N. Superstructures of Chiral Nematic Microspheres as All-Optical Switchable Distributors of Light. *Sci. Rep.* **2015**, *5* (1), 14183.
(56) Noh, J.; Reguengo De Sousa, K.; Lagerwall, J. P. F. Influence of Interface Stabilisers and Surrounding Aqueous Phases on Nematic Liquid Crystal Shells. *Soft Matter* **2016**, *12* (2), 367−372.
(57) Zhang, Z.; Zhang, Z.; Chang, T.; Wang, J.; Wang, X.; Zhou, G. Phase Change Material Microcapsules with Melamine Resin Shell via Cellulose Nanocrystal Stabilized Pickering Emulsion In-Situ Polymerization. *Chem. Eng. J.* **2022**, *428*, 131164.
(58) Siegwardt, L.; Gallei, M. Complex 3D-Printed Mechanochromic Materials with Iridescent Structural Colors Based on Core-Shell Particles. *Adv. Funct Materials* **2023**, *33* (15), 2213099.
(59) Zhu, Y.; Liu, Y.; Hu, H.; Xu, Z.; Wu, C.; Kim, D. H.; Guo, T.; Li, F.; Kim, T. W. Intelligent, Biomimetic, Color-Tunable, Light-Emitting Artificial Skin with Memory Function. *Nano Energy* **2021**, *90*, 106569.

https://doi.org/10.1021/prechem.4c00103
Precis. Chem. 2025, 3, 149−156